Tribology Transactions

ISSN: 1040-2004 (Print) 1547-397X (Online) Journal homepage: http://www.tandfonline.com/loi/utrb20

The Measurement and Study of Very Thin Lubricant Films in Concentrated Contacts

G. J. Johnston , R. Wayte & H. A. Spikes

To cite this article: G. J. Johnston , R. Wayte & H. A. Spikes (1991) The Measurement and Study of Very Thin Lubricant Films in Concentrated Contacts, Tribology Transactions, 34:2, 187-194, DOI: 10.1080/10402009108982026

To link to this article: http://dx.doi.org/10.1080/10402009108982026

Published online: 25 Mar 2008.

Submit your article to this journal

Article views: 493

View related articles

Citing articles: 327 View citing articles

Full Terms & Conditions of access and use can be found at
http://www.tandfonline.com/action/journalInformation?journalCode=utrb20

Download by: [Technische Informationsbibliothek (TIB)] **Date:** 05 November 2017, At: 01:09

VOLUME 34 (1991), 2, 187–194
TRIBOLOGY TRANSACTIONS

The Measurement and Study of Very Thin Lubricant Films in Concentrated Contacts©

G. J. JOHNSTON, R. WAYTE and H. A. SPIKES (Member, STLE)
Imperial College
London, England SW7 2BX

Downloaded by [Technische Informationsbibliothek (TIB)] at 01:09 05 November 2017

Optical interferometry is now a widely used technique for measuring the separating film thickness in model rolling and sliding elastohydrodynamic contacts. There are two limitations of the method as conventionally employed: first, it cannot easily be used to accurately measure films less than one quarter the wavelength of visible light, i.e. less than about 100 nm. Secondly, only certain, discrete thicknesses, spaced at least 50 nm apart can be determined. This paper describes work aimed at overcoming these limitations so as to make optical interferometry applicable to the study of boundary or very thin film elastohydrodynamic lubrication in rolling contacts. A combination of a solid spacer layer with spectrometric analysis of reflected light from the contact enables very thin lubricant films to be accurately measured. The approach is applied to the study of thin films formed in rolling contacts by low viscosity lubricants. Some anomalies in the relationship between film thickness and speed are found with films of less than 15 nm thickness.

INTRODUCTION

The primary role of a lubricant is generally to reduce friction at the interface of two rubbing surfaces. Liquid lubricants achieve this by forming a film which separates the surfaces and thus limits their contact and adhesion. The film formed can vary in thickness from just a few monolayers of adsorbed or chemically reacted material, the regime of boundary lubrication, to hundreds of thousands of nanometers of hydrodynamically entrained lubricant, as is found in the elastohydrodynamic (EHD) and hydrodynamic lubrication regimes.

It is of considerable practical importance to be able to measure the thickness of lubricant films in contacts, both in order to test predictive theories and also to assess the effectiveness of lubricants. A number of experimental methods have therefore been developed, based mainly upon electrical or electromagnetic radiation measurements, to determine film thickness in hydrodynamic and EHD contacts. In EHD, the technique of optical interferometry has been particularly successful in measuring films in the range of 100 to 1000 nm (*1*).

It has proved difficult, however, to devise accurate techniques for looking at films thinner than 100 nm. This is unfortunate since many practical lubricated systems operate with such thin films, especially at high temperatures and thus low oil viscosities. It is also of interest to learn what happens to the film-generating capability of lubricant at the borderline between EHD and boundary lubrication and, indeed, below it. EHD theory is based upon continuum fluid mechanics and there must come a point, as film thickness diminishes, when the theory ceases to be valid simply because there are insufficient molecules of oil in the film to maintain a realistic continuum. Currently, workers are studying this borderline by either applying modified quasi-continuum fluid models (*2*) or by molecular dynamics simulation (*3*). However such models are being developed in the absence of supportive experimental data.

This paper describes the development and application of an extension of conventional optical interferometry which allows separating films in rolling point contacts to be measured accurately well below 100 nm, down to less than 5 nm. The technique is then applied to a study of the film-forming abilities of several lubricants at very low speeds and of low-viscosity fluids at moderate speeds.

FILM THICKNESS MEASUREMENT— OPTICAL INTERFEROMETRY

A number of methods have been developed for measuring lubricant film thickness in EHD and hydrodynamic contacts. Table 1 lists the most common ones. Capacitance has been the most widely-used method for looking at film thickness in realistic metal-metal contacts in service test equipment such as bearings (*12*) and piston liner/rings (*13*), whereas optical interferometry has proved most valuable for studying lubricants and their ability to generate EHD films in model contacts.

Presented at the 45th Annual Meeting
In Denver, Colorado
May 7–10, 1990
Final manuscript approved April 5, 1990

Downloaded by [Technische Informationsbibliothek (TIB)] at 01:09 05 November 2017

TABLE 1—METHODS OF MEASURING OIL FILM THICKNESS

METHOD	REFS.
Capacitance	(4) (5)
Resistance	(6)
Voltage Discharge	(7)
Optical Interferometry	(1)
X-Ray	(8)
Fluorescence	(9)
Colorimetric Absorption	(10)
Inductance	(11)

The principle of optical interferometry is shown in Fig. 1(a). One surface of a lubricated contact is highly reflective, usually a smooth steel ball or roller, but the other is made of a material transparent to visible light, generally glass or sapphire. This surface is normally coated with a thin, semi-reflective layer. When light is shown through the glass it undergoes a division of amplitude, with one beam reflecting directly back from the semi-reflective layer on the underside of the glass but the other passing through the lubricant film before being reflected back from the steel. This latter beam has thus travelled two oil film thicknesses further than the former so that the two beams are out of phase and on recombination they interfere, constructively or destructively, according to the equations:

destructive interference

$$h_{oil} = \frac{\left(N + \frac{1}{2} - \phi\right)\lambda}{2\, n \,\mathrm{Cos}\,\theta} \qquad N = 0,1,2 \qquad [1]$$

constructive interference

$$h_{oil} = \frac{(N - \phi)\lambda}{2\, n \,\mathrm{Cos}\,\theta} \qquad N = 1,2,3 \qquad [2]$$

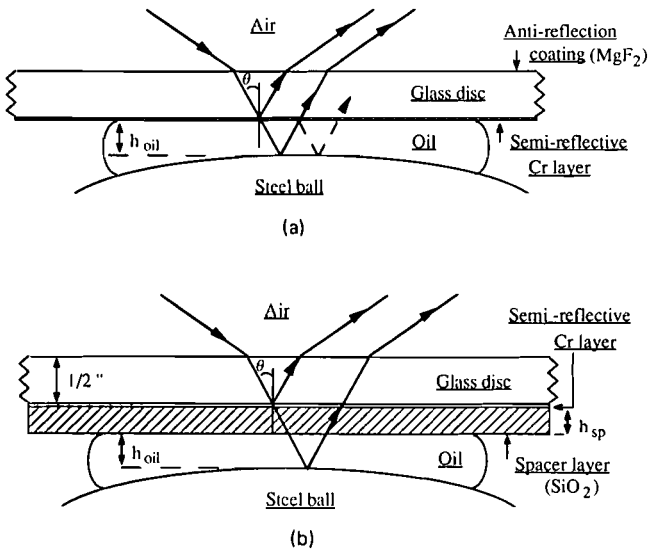

Fig. 1—(a) Basic interferometric method (two beam). (b) Spacer layer method.

h_{oil} is the spatial thickness of the oil film i.e. the optical film thickness divided by the oil refractive index, n, λ is the wavelength, θ is the angle of incidence of the beam (usually 0°), ϕ is any net phase change that occurs upon reflection and N is the fringe order.

The phase change, ϕ, can be found by calibration from a static contact (*14*). The refractive index of the oil at the high pressure in the contact is required to determine spatial film separation. This is generally obtained by applying a small pressure correction to the refractive index measured at atmospheric pressure (*14*), but it can also be measured directly using two-angle interferometry (*15*). An increase in pressure from atmospheric to 1 GPa has been shown to alter n by less than 10 percent (*15*). In the current study the maximum Hertz pressure was approximately 0.45 GPa; the refractive indices quoted were measured at atmospheric pressure and the test temperature of 24.5 ± 0.5°C.

Monochromatic light can be used, in which case dark and light interference fringes, representing the separation of the glass and steel over the area viewed, are obtained. Alternatively duochromatic or white light can be employed to give more complex interference fringe patterns. In the latter case, a set of separation-dependent, colored interference fringes is obtained from the combination of all the component wavelengths of light which interfere either constructively or destructively. The thickness-fringe color relationship then has to be obtained by calibration. The result of a typical calibration is shown in Table 2.

Optical interferometry produces an interference fringe pattern which provides a detailed map of surface separation over the area viewed. The disadvantage of optical interferometry over electrical techniques is clearly that one surface must be made of glass or sapphire, so that the method cannot easily be applied to realistic machine systems.

One advantage of optical interferometry over capacitance is that the former requires a knowledge of refractive index of the material in the contact whereas the latter needs the dielectric constant. Refractive indices of organic materials span a much narrower range of values than do dielectric constants and are far less susceptible to variations in the composition of the film material.

There are two important limitations of conventional optical interferometry of lubricated contacts as outlined above.

TABLE 2—FRINGES OBSERVED IN CHROMATIC INTERFEROMETRY

	COLOR	SEPARATION/(nm)*
FIRST ORDER	Yellow	139
	Red	188
	Blue	236
	Green	299
SECOND ORDER	Yellow	326
	Red	389
	Blue	424
	Green	465

*Assumes refractive index of oil = 1.44

Downloaded by [Technische Informationsbibliothek (TIB)] at 01:09 05 November 2017

One can be seen from Eq. [1]. In monochromatic interferometry the first destructive interference fringe occurs at typically 74.3 nm in air and 53.0 nm in oil, using a red source for which λ is approximately 675 nm. These values were calculated from Eqs. [1] and [2] using a net phase change of 0.28, an angle of incidence of 0° and $n_{oil} = 1.4$. The identification of destructive interference using monochromatic interferometry is however limited by the relatively poor ability of the human eye to determine intensity levels. With chromatic interferometry the minimum observable separation occurs as a constructive fringe at approximately 200 nm in air and 130 nm in oil and this represents the minimum film thickness easily measurable by the method. The minimum can be brought down slightly by using an angle of incidence greater than 0° but total internal reflection limits any further reduction (*16*).

The most successful approach to overcoming this limitation, which has been adopted in this study, is shown schematically in Fig. 1(b). A coating of transparent solid, typically silica, of known thickness, is deposited on top of the semi-reflecting layer. This solid thus permanently augments the thickness of any oil film present and is known as a "spacer layer." Hence destructive interference now obeys the equation:

$$n_{oil}h_{oil} + n_{sp}h_{sp} = \frac{\left(N + \frac{1}{2} - \phi\right)\lambda}{2 \text{ Cos } \theta} \qquad N = 0,1,2, \quad [3]$$

and the first interference fringe occurs at a separation reduced by h_{sp}, where h_{sp} is the spatial thickness of the spacer layer. With a flat spacer layer, Westlake was able to measure an oil film of only 10 nm thickness using optical interferometry (*17*).

The use of a spacer layer does not overcome the second problem of optical interferometry which is the limited resolution and accuracy of film thickness measurement. This limitation can be seen in Table 2, which shows that the thicknesses that can be measured are 50 nm apart and, due to the inability of human beings to perceive colors precisely and accurately, are ± 20 nm. When monochromatic interferometry is used, resolution is worse, at λ/4, although multiple beam interferometry does provide very high precision.

This poor resolution obviates the value of spacer layers since there is little point in measuring an initial film thickness of 10 nm if the next thickness that can be measured is 60 nm.

One method of overcoming this limitation has recently been described by Guangteng and Spikes (*18*). They used an alumina spacer layer whose thickness varied in the shape of a wedge over the transparent flat surface in an optical rig. This meant that, with no oil film present, fringes were produced at certain locations ont he surface where the spacer layer was an appropriate thickness to cause interference. However, when a thin oil film was formed it had the effect of moving these interference fringes a short distance, to a position of lower thickness spacer layer. Measurement of fringe movement then yielded oil film thickness. The method was able to detect oil film thickness down to less than 10 nm. A problem encountered using this technique was the difficulty of obtaining regular spacer layer wedges. Also, with low viscosity oils, requiring high speeds to generate films, high speed recording equipment was needed to chart the continuously changing interference fringe colors.

To overcome these problems a new experimental approach has been devised and is reported in this paper.

CURRENT EXPERIMENTAL APPROACH

In this study, the two limitations of optical interferometry, the one-quarter wavelength of light limit and the low resolution, have been addressed by using a combination of a fixed-thickness spacer layer and spectral analysis of the reflected beam. The first of these overcomes the minimum film thickness that can normally be measured and the second addresses the limited resolution of conventional chromatic interferometry. This combination has been used in force balance instruments, where mica surfaces provide an effective spacer layer (*19*) but has not previously been applied to realistic lubricated contacts.

A conventional optical test rig was employed, as shown in Fig. 2. A 25.4 mm diameter superfinished steel ball is loaded against the flat surface of a float-glass disc. Both surfaces can be independently driven, although in most of the work described in this paper the ball was driven by a shaft and the disc was driven, in nominally pure rolling, by the ball.

The disc was coated with a 20 nm sputtered chromium semi-reflecting layer, and for this study, a silica spacer layer was sputtered on top of this chromium. This spacer layer varied in thickness in the radial direction, but was approximately constant circumferentially round the disc (so that as the disc rotates the contact sees a near-constant thickness). The image captured for spectral analysis was triggered by the disc rotation so that all spectra in a series could be taken from the same position on the disc circumference.

In conventional optical interferometry the position and color of interference fringes is noted by eye. In the current study the reflected beam was taken through a narrow, rectangular aperture arranged parallel to the rolling direction,

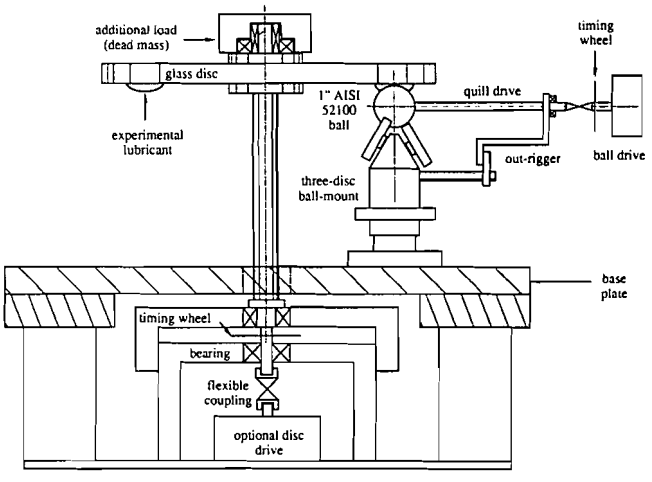

Fig. 2—Schematic representation of optical EHD rig.

Downloaded by [Technische Informationsbibliothek (TIB)] at 01:09 05 November 2017

as shown in Fig. 3(a). It was then dispersed by a spectrometer grating and the resultant spectrum captured by a black and white video camera. This produced a band spectrum spread horizontally on a television screen, with the brightness of the spectrum at each wavelength indicating the extent of interference, as shown schematically in Fig. 3(b). The vertical axis of the spectral band mapped across the center of the contact as illustrated in Fig. 3(a). This image was screen-dumped in digital form into a microcomputer which drew an intensity profile of the spectrum as a function of wavelength. This is shown in Fig. 3(c). In practice the spectrometer was arranged so that one digitized screen pixel corresponded to a wavelength change of 0.48 nm.

To obtain high spectral resolution, the magnification was such that only a portion of the spectrum fit on the screen. The spectrometer grating was rotated using a micrometer to scan the whole spectrum, which was calibrated with respect to micrometer reading and screen position by passing the light from a mercury lamp, with known wavelength emission, into the spectrometer. In test work a cold halogen white light source was employed. In all work the angle of incidence was 0°.

By this means, the wavelength of light which constructively interfered could be determined accurately for any separating film thickness, thus permitting a highly resolved film thickness measurement.

Table 3 summarizes the test condition employed in this study and Table 4 lists the lubricants used. Siloxane A has 50 percent phenylmethyl and 50 percent methylmethyl units. Siloxane B has only 10 percent phenylmethyl.

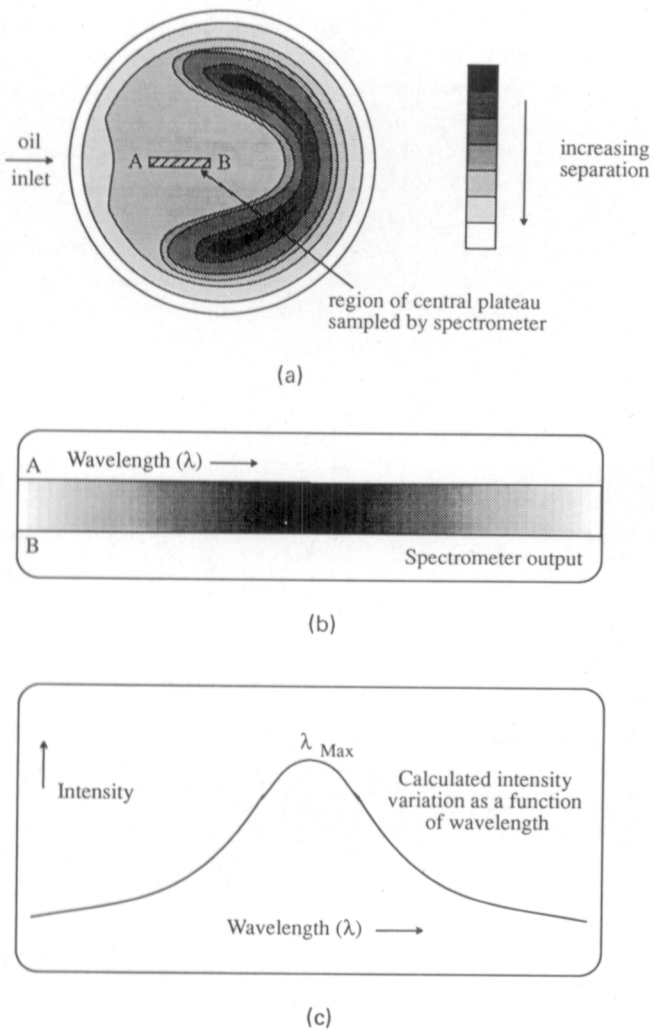

Fig. 3—(a) Schematic map of EHD point contact showing region observed by spectrometer.
(b) Schematic representation of screen display showing spectrometer output.
(c) Schematic representation of screen display showing calculated intensity profile.

RESULTS

Spacer Layer Thickness Effect

Initial work used a disc sputtered with a relatively thin silica spacer layer of approximately 100 nm. The thickness of silica was determined in two ways. When the spacer layer was sputtered, a thin radial strip of the disc was masked, so that a shallow silica-free groove was obtained. The thickness of silica on either side of this was then measured by passing a talysurf stylus across the groove in a circumferential direction. The spacer layer thickness was measured as a function of the disc radius. The results are shown in Fig. 4(a).

The silica film thickness was also determined, as a function of the disc radius, by an optical interference method, using the spectrometer. A steel ball was loaded against the silica surface to obtain an interference pattern of a central, circular Hertzian area with surrounding circular fringes due to the air gap between deformed ball and flat. The thickness of the silica layer in the Hertzian contact was calculated from the measured wavelength at which maximum constructive interference occurred, λ_{max}, by solving Eq. [4] for h_{sp}. N was known from the approximate thickness of the silica layer and ϕ was taken to be 0.28 from the value measured previously in air. The refractive index of the separating medium is known to affect ϕ by less than 2 percent (*20*). The refractive index of the spacer layer, n_{sp}, was measured as 1.476 ± 0.001 by the method of Kauffman (*21*).

$$h_{sp} = \frac{(N - \phi)\lambda_{max}}{2\, n_{sp}} \qquad [4]$$

Using the thin silica spacer layer it was found that the two calibration methods did not agree, as shown in Fig. 4(a). This was tentatively ascribed to the effect of penetration of the reflecting beam into the substrate. With a very thin silica layer, the depth of penetration and thus the phase change would depend upon the thickness of the silica spacer layer and also upon that of any oil film present.

The solution to this problem was to use a spacer layer of thickness greater than the wavelength of visible light, which is above the limit of penetration of a reflected light beam.

TABLE 3—EXPERIMENTAL CONDITIONS

Load	23 N
Max. Hertz pressure	0.445 GPa
Speed range	0.0034–0.13 ms^{-1}
Temperature	24.5 ± 0.5°C

Downloaded by [Technische Informationsbibliothek (TIB)] at 01:09 05 November 2017

TABLE 4—MEASURED VISCOSITIES AND REFRACTIVE INDICES FOR EXPERIMENTAL LUBRICANTS

LUBRICANT	VISCOSITY/(Pa.s) (24.5 ± 0.5°C)	REFRACTIVE INDEX
Mineral oil	0.364	1.4868
Liquid crystal (E 44)*	0.0448	1.5270
Squalane	0.0302	1.4498
tri-tolyl phosphate	0.0758	1.5535
Synthetic hydrocarbon (PAO)	0.0497	1.4570
Methyl phenyl siloxane—A	0.1536	1.4974
Methyl phenyl siloxane—B	0.0546	1.4225
Type II (polyol) ester	0.0349	1.4516
Hexadecane	0.0030	1.4323

*Eutectic cyano alkyl biphenyl

Any variation above this value, due to spacer layer or oil, will have no further effect on phase change. Figure 4(b) shows that with a thick spacer layer there was good agreement between talysurf and optical calibration methods, and this thick spacer layer was employed in subsequent work.

Validation of the Technique

Two experiments were undertaken to validate the experimental technique. In the first, the spectrometer was tested by carrying out film thickness measurements at a range of rolling speeds with mineral oil using (1) conventional color-recognition chromatic optical interferometry and (2) the spectrometer method of wavelength measurement. A conventional disc coated only with a semi-reflective chromium coating was used. The oil film thickness was calculated from λ_{max} as in the solution of Eq. [4] for h_{sp} above. Figure 5 shows the good agreement between the two methods and illustrates how many more data points the spectrometer can provide than the color-recognition method. When the spectrometer was used without a spacer layer each set of measurements for a given fringe order appeared to cross rather than exactly parallel the overall film thickness line. This may result from a dependence of phase change on film thickness at film thicknesses less than a wavelength of light mentioned above. This effect is not seen with thicker films or with a thick spacer layer present.

A comparison was also carried out on the same oil using (1) the spectrometer without a spacer layer and (2) the spectrometer with a spacer layer on the disc. With the spacer layer present the oil film thickness (h_{oil}) is calculated according to Eq. [7], from the spacer layer thickness (h_{sp}) measured with the disc stationary, Eq. [5] and the combined spacer layer plus oil film thickness ($h_{sp} + h_{oil}$) at a given rolling speed, Eq. [6]. Figure 6 shows, again, good agreement between the measurements made with the two methods and indicates the much lower film thicknesses measurable using the spacer layer. With this, quite viscous oil, the film thickness measured was constrained by the lowest speed attainable on the test rig. The film thicknesses measured for the mineral oil were indistinguishable from those calculated from EHD theory. The mineral oil had a viscosity of 0.364 Pa.s and an effective pressure-viscosity coefficient (α value) of 21.75 GPa^{-1} at the test temperature of 24.5 ± 0.5°C.

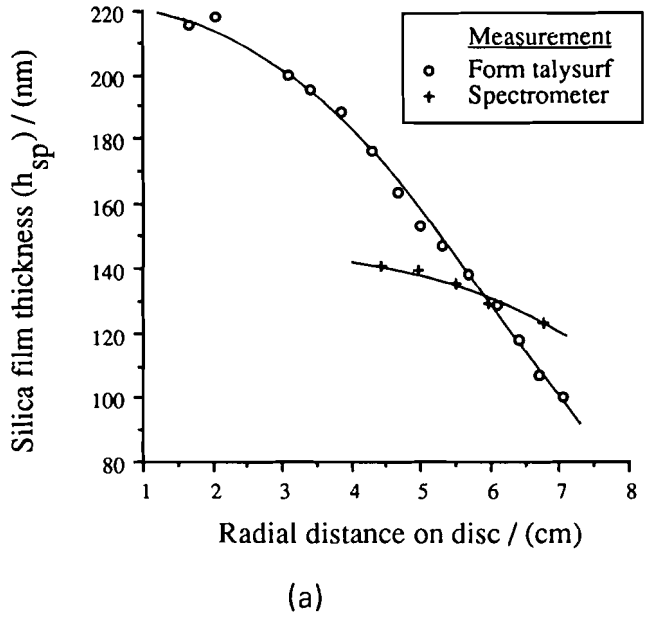

Fig. 4—(a) Measured film thickness—thin spacer layer. (b) Measured film thickness—thick spacer layer.

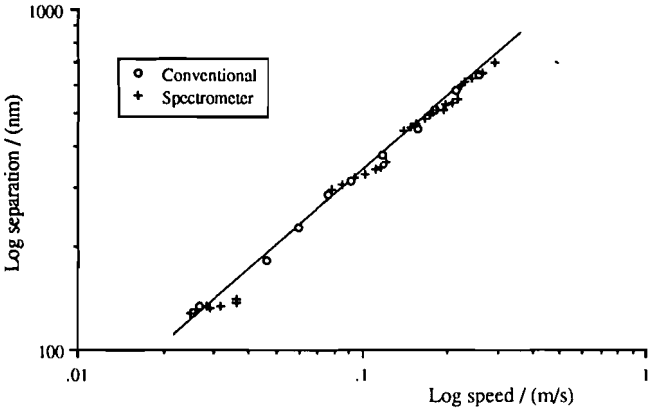

Fig. 5—Log separation *vs.* log speed measured conventionally and using spectrometer on an uncoated disc—mineral oil.

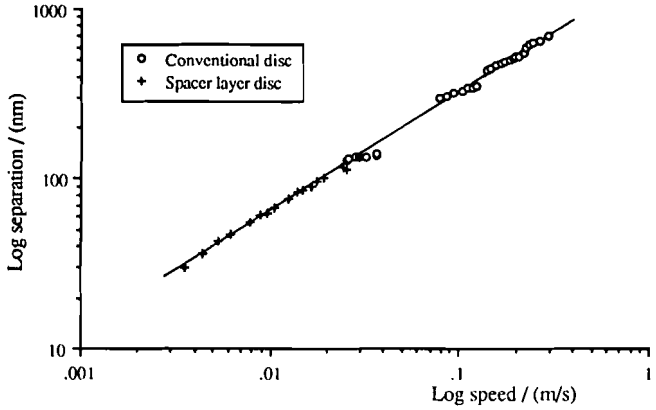

Fig. 6—Log separation *vs* log speed measured using spectrometer on an uncoated disc and a spacer layer disc—mineral oil.

$$2\,n_{sp}h_{sp} = (N_{sp}-\phi)\lambda_{sp} \quad [5]$$

$$2\,n_{sp}h_{sp} + 2\,n_{oil}h_{oil} = (N_{sp+oil}-\phi)\lambda_{sp+oil} \quad [6]$$

$$h_{oil} = \left[\frac{((N_{sp+oil}-\phi)\lambda_{sp+oil} - (N_{sp}-\phi)\lambda_{sp})}{2\,n_{oil}}\right] \quad [7]$$

Results for Different Lubricants

Figures 7–10 show logarithmic plots of film thickness *vs.* rolling speed for eight fluids tested using the combined spacer layer/spectrometer system. Each point in Figs. 7–9 represents an average of at least three measurements. The results indicate that the method can currently measure film thicknesses reliably down to approximately 5 nm. With more viscous fluids these film thicknesses could not be reached because the test rig was unable to run at sufficiently low speed. It is considered that the results are ±2 nm but, for Fig. 10, where more measurements were taken at each speed, results are ±1 nm.

DISCUSSION

The results show that all fluids tested obey quite closely the well-known elastohydrodynamic relationship between central film thickness, h_{oil}, and entrainment velocity U:

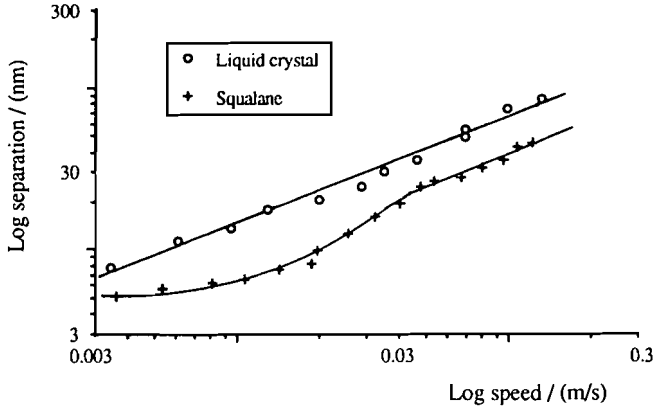

Fig. 7—Log separation *vs.* log speed—Liquid crystal (E44) and squalane.

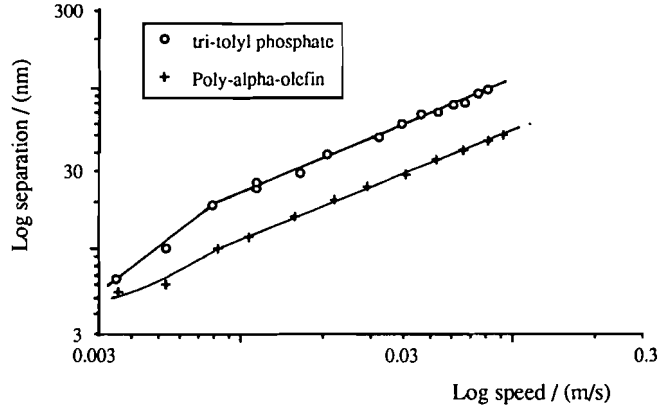

Fig. 8—Log separation *vs.* log speed—*tri*-tolyl phosphate and synthetic hydrocarbon (PAO).

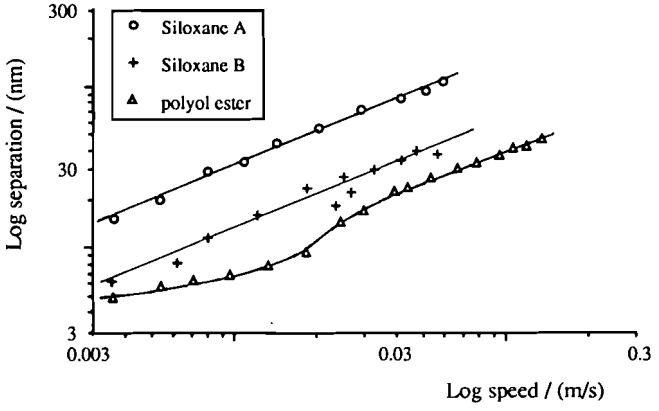

Fig. 9—Log separation *vs.* log speed—methyl phenyl siloxane A, methyl phenyl siloxane B and type II (polyol) ester.

$$h = k_1 U^{0.7} \quad [8]$$

down to a film thickness of 15 nm. By comparing the film thicknesses obtained for the fluids tested with those of the reference mineral oil, of known viscosity and pressure viscosity coefficient, it was possible to determine the effective pressure viscosities, α, of the former from the EHD equation:

$$h = k_2 U^{0.7}\eta^{0.7}\alpha^{0.5} \quad [9]$$

Downloaded by [Technische Informationsbibliothek (TIB)] at 01:09 05 November 2017

Downloaded by [Technische Informationsbibliothek (TIB)] at 01:09 05 November 2017

where η is the atmospheric dynamic viscosity of the fluid. Table 5 summarizes the pressure viscosity coefficients obtained. The values were calculated at the fixed value of log $(U.\eta) = -2.5$ N/m as described in (*14*). Table 5 includes the gradients of the best fit lines drawn through the log h *vs.* log U plots and a list of α values obtained from the literature for similar fluids. As can be seen these compare well with values from either conventional optical interferometry or from high pressure viscometry.

Below 15 nm there appear to be some anomalous film thickness effects. With squalane, tritolylphosphate, and the polyol ester there was evidence of an increased dependence of film thickness on rolling speed in the range 5–15 nm. This was not seen with the liquid crystal. With the synthetic hydrocarbon and the low viscosity silicone an effect was observed but was it within error estimates.

The reason for this effect is not clear. It may originate from a breakdown in the continuum assumption used in hydrodynamic theory although, in this context, it must be remembered that an EHD film is generated at the inlet where the film thickness is slightly greater than the central film thickness.

One possibility is that, with very thin films, fluid ordering near the surfaces produces molecular alignment which results in the fluid having an effective viscosity less than its bulk value. Thus, in the range 5 to 15 nm the loss of this non-Newtonian effect might be seen as the move towards the bulk fluid properties is made. Viscosity reductions near surfaces have been observed by Derjaguin using the oil film blow off technique and, for a diacid ester, occur at between 10 and 15 nm (*25*). Further study is needed to confirm and further investigate this effect.

With the low viscosity fluids squalane and polyol ester, there was evidence of a residual separating film of approximately 5 nm thickness, which was almost speed-independent. This film disappeared however, when rolling was completely halted.

The current rig could not be run at sufficiently low speed to see whether a similar effect occurred with the other fluids. Very much clearer evidence of the phenomenon can be seen in Fig. 10, which shows the result of two tests, with purified hexadecane and with a saturated solution of stearic acid in hexadecane. These results are at the limit of resolution of the method but shows that purified hexadecane gave no

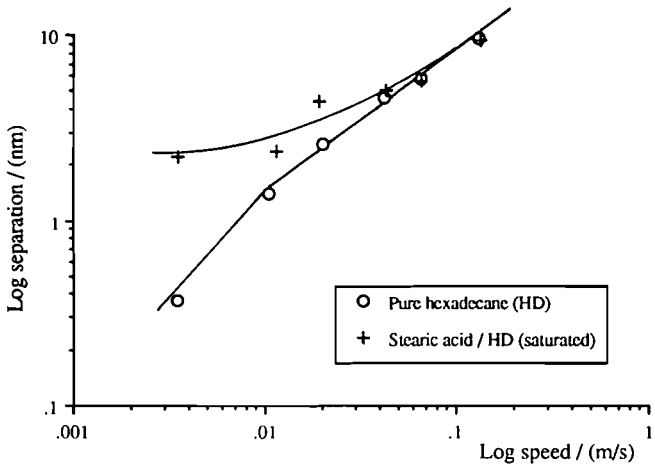

Fig. 10—Log separation *vs.* log speed—purified hexadecane ± stearic acid.

apparent residual film. (The very low film thickness measurement for hexadecane was an average of six readings and is believed to be 1 nm ± 1 nm). However the stearic acid solution appeared to give a separation of about 2 nm, which persisted down to very low speeds, although it disappeared when rolling was halted.

The authors tentatively ascribe this effect to an absorbed film of stearic acid on one or both surfaces. The height of an upright, aligned stearic acid molecule is approximately 2.5 nm, (*26*) but little is known about its likely orientation under a Hertzian contact pressure. If this interpretation is correct, then it must be inferred that the absorbed film cannot persist on surfaces under static contact pressures but is squeezed off. This interpretation is by no means the only one. The effect may be due to a viscous surface film of polar material. Further study, after refinement of the experimental technique, should help elucidate the matter. It is interesting to note that, as speed increases and a hydrodynamic film is generated, the residual 2 nm film thickness due to the stearic acid does not appear to continue to augment the film thickness of the fluid. The reason for this is not understood but may result from a boundary shear effect at high speeds or from localized heating and desorption in the inlet.

In the above discussion, the possible effects of surface roughness have not been considered. The root mean square

TABLE 5—MEASURED AND LITERATURE PRESSURE-VISCOSITY COEFFICIENTS

LUBRICANT	CALCULATED α VALUE/(GPa^{-1})	PREVIOUS α VALUE/(GPa^{-1})*	EHL SPEED EXPONENT
Mineral oil	21.75	21 (*22*)	0.71
Liquid crystal (E 44)	17.1	—	0.66
Squalane	9.52	14 (*13*)	0.69
tri-tolyl phosphate	22.5	19 (*22*)	0.69
Synthetic hydrocarbon (PAO)	10.8	—	0.70
Methyl phenyl siloxane—A	18.3	21 (*23*)	0.69
Methyl phenyl siloxane—B	12.0	14.5 (*23*)	0.68
Type II (polyol) ester	8.5	7.5 (*22*)	0.68
Hexadecane	10.6	8 (*24*)	0.69

*Similar basestocks (references in brackets)

roughness of the ball and the silica surface were 0.01 and 0.0004 μm respectively, giving a composite surface roughness of 11 nm. However it must be noted that this is an out-of-contact value. Elastic flattening will greatly reduce this. It is difficult to predict the effect on film thickness of load being carried by asperities. The fluid pressure in the inlet will drop, and this will reduce the inlet viscosity and thence the film-generating capabilities of the lubricant. However this will be counter-balanced by the fact that the contacting asperities will, themselves, help hold the surface apart. A further possible explanation for the change in gradient of log h against log U for some fluids tested is that it represents a transition from EHD to isoviscous lubrication as load is borne by contacting asperities, thus reducing the oil pressure in the inlet.

However, in view of the fact that the anomalous film thickness effects below 15 nm were fluid dependent, the authors currently do not consider them to originate directly from surface roughness.

CONCLUSIONS

The technique of optical interferometry has been extended so that it can measure separating films between rolling steel ball on glass surfaces down to less than 5 nm. Work is currently taking place to reduce this limit and to increase the accuracy of measurements by using automatic, multiple sampling techniques and multiple beam interferometry. The importance of surface roughness is being investigated by using steel balls of variable roughnesses.

It has been shown that standard circular contact EHD film thickness equations can be used with a range of fluids to predict central film thickness down to 15 nm.

For some fluids, the film thickness generated in the range 5 to 15 nm appears to be more speed-dependent than EHD theory predicts.

With some hydrocarbon fluids and with a solution of stearic acid in hexadecane, there is evidence of a residual surface film between 2 and 5 nm thick in rolling contacts that persists down to very low speeds. This film, which is tentatively ascribed to adsorbed material, does not withstand the pressures of a static Hertzian contact.

REFERENCES

(1) Gohar, R. and Cameron, A., "The Mapping of Elastohydrodynamic Contacts," *ASLE Trans.*, **10,** pp 215–225 (1967).

(2) Dickinson, P. J., "Polymer Modified Oils in Elastohydrodynamic Lubrication," Ph.D. Thesis, University of London (1982).

(3) Brown, D. and Clarke, J. H. R., "The Rheological Properties of Model Liquid n-Hexane Determined by Non-Equilibrium Molecular Dynamics," *Chem. Phys. Letters*, **98,** pp 579–583 (1983).

(4) Crook, A. W., "The Lubrication of Rollers I," *Phil. Trans. Roy. Soc.*, **A250,** pp 387–409 (1987).

(5) Alliston-Greiner, A. F., Greenwood, J. A. and Cameon, A., "Thickness Measurements and Mechanical Properties of Reaction Films Formed by ZDDP During Running," *I. Mech. E.* C178/87, pp 565–572, International Conference, "Tribology-Friction, Lubrication and Wear, Fifty Years On," (1987).

(6) Wilson, R. W., "The Contact Resistance and Mechanical Properties of Surface Films on Metals," *Proc. Phys. Soc.*, **68B,** pp 625–641 (1955).

(7) Cameron, A., "Surface Failure in Gears," *Jour. Inst. Pet.*, **40,** pp 191–196 (1954).

(8) Kimura, Y. and Okade, K., "Film Thickness at Elastohydrodynamic Conjunctions Lubricated with Oil-in-Water Emulsions," *I. Mech. E.* C176/87, pp 85–89, International Conference, "Tribology-Friction, Lubrication and Wear, Fifty Years On," (1987).

(9) Hoult, D. P., Lux, J. P., Wong, V. W. and Billian, S. A., "Calibration of Laser Fluorescence of Film Thickness in Engines," *SAE Tech. Ser.* **881587,** Int. Fuels and Lub. Meeting, pp 1–9 (1988).

(10) Wordsworth, R. A., "Incomplete Oil Films in Journal Bearings: An Optical Study," Ph.D. Thesis, Univ. of Lond. (1983).

(11) Wing, R. D. and Saunders, O. A., "Oil Film Temperature and Thickness Measurements on the Piston Rings of a Diesel Engine," *Proc. I. Mech. E.*, **186,** pp 1–9 (1972).

(12) Safa, M. M. A., Anderson, J. C. and Leather, J. A., "Transducers for Pressure, Temperature and Oil Film Thickness Measurements in Bearings," *Sensors and Actuators*, **3,** pp 119–128 (1982–83).

(13) Moore, S. L., "The Effect of Viscosity Grade on Piston Ring Wear and Film Thickness in Two Particular Diesel Engines," *I. Mech. E.* C184/87, pp 473–482, International Conference, "Tribology-Friction, Lubrication and Wear, Fifty Years On," (1987).

(14) Foord, C. A., Hamman, W. C. and Cameron, A., "Evaluation of Lubricants Using Optical Elastohydrodynamics," *ASLE Trans.*, **11,** pp 31–43 (1968).

(15) Paul, G. R. and Cameron, A., "An Absolute High Pressure Microviscometer Based on Refractive Index," *Proc. Roy. Soc. Lond.*, **A331,** pp 171–184 (1984).

(16) Liang, X. and Linqing, Z., "A New Method for the Experimental Investigation of Contacts in Mixed Lubrication," *Wear*, **132,** pp 221–233 (1989).

(17) Westlake, F. J., "An Interferometric Study of Ultra-Thin Fluid Films," Ph.D. Thesis, Univ. of London (1970).

(18) Guangteng, G. and Spikes, H. A., "Properties of Ultra-Thin Lubricating Films Using Wedged Spacer Layer Optical Interferometry," *Proc. 14th Leeds-Lyon Symp. on Trib., "Interface Dynamics,"* pp 275–279, ed Dowson, D., Elsevier (1988).

(19) Horn, R. G., Israelichvili, J. N. and Perez, E., "Forces Due to Structure in a Thin Liquid Crystal Film," *Jour. Physique*, **42,** pp 39–52 (1981).

(20) Wedeven, L., "Optical Measurements in Elastohydrodynamic Rolling Contacts," Ph.D. Thesis, Univ. of London (1970).

(21) Kauffman, A. M., "A Simple Immersion Method to Determine the Refractive Index of Thin Silica Films," *Thin Solid Films*, **1,** pp 131–136 (1967).

(22) Spikes, H. A., Cann, P. and Caporiccio, G., "Elastohydrodynamic Film Thickness Measurements of Perfluoropolyethers," *Jour. Synth. Lubr.*, **1,** pp 73–86 (1984).

(23) Kuss, E., "Viskositats-Druckverhalten von flüssigen Methyl-Phenylmethyl- und Cyclohexylmethyl-Siloxeanen," *Erdöl und Kohle-Erdgas-Petrochemie vereinigt mit Brennstoff-Chemie*, **27,** 8, pp 416–422 (1974).

(24) Duocoulombier, D., Zhou, H., Bonded, C., Peyrelase, J., Saint-Guirons, H. and Xans, P., "Pressure (1–1000 bars) and Temperature (20–100°C) Dependence of the Viscosity of Liquid Hydrocarbons," *Jour. Phys. Chem.*, **90,** pp 1692–1700 (1986).

(25) Akhmatov, A. S., *Molecular Physics of Boundary Friction*, Israel Prog. for Sci. Transl., Jerusalem (1966) chapt. 8.

(26) Cameron, A., *Basic Lubrication Theory*, 3rd. Edition., Ellis Horwood, Chichester (1981) chapt. 15.

Downloaded by [Technische Informationsbibliothek (TIB)] at 01:09 05 November 2017